Supporting information

Crystal engineering of conglomerates: Dilution of racemate-forming Fe(II) and Ni(II) congeners into conglomerate-forming $[Zn(bpy)_3](PF_6)_2$

Table S1. Crystal data and structure refinement for [Λ-$Zn(bpy)_3$]$(PF_6)_2$ and [*rac*-$Ni(bpy)_3$]$(PF_6)_2$

Empirical formula	$C_{30}H_{24}F_{12}N_6P_2Zn$	$C_{30}H_{24}F_{12}N_6NiP_2$
Formula weight	823.86	817.187
Temperature/K	296.15	296.15
Crystal system	trigonal	trigonal
Space group	$P3_2$	P-3c1
a/Å	10.4744(7)	10.7527(4)
b/Å	10.4744(7)	10.7527(4)
c/Å	26.395(3)	16.5475(10)
α/°	90	90
β/°	90	90
γ/°	120	120
Volume/Å^3	2507.9(4)	1656.91(13)
Z	3	2
ρ_{calc}g/cm^3	1.637	1.638
μ/mm^{-1}	0.930	0.783
F(000)	1242.0	825.7
Crystal size/mm^3	0.32 × 0.23 × 0.14	0.4 × 0.15 × 0.12
Radiation	MoKα (λ = 0.71073)	Mo Kα (λ = 0.71073)
2Θ range for data collection/°	1.542 to 56.606	6.58 to 56.66
Index ranges	-13 ≤ h ≤ 13, -13 ≤ k ≤ 13, -35 ≤ l ≤ 35	-14 ≤ h ≤ 14, -14 ≤ k ≤ 14, -22 ≤ l ≤ 22
Reflections collected	141892	73292
Independent reflections	8163 [R_{int} = 0.0289, R_{sigma} = 0.0109]	1365 [R_{int} = 0.0266, R_{sigma} = 0.0057]
Data/restraints/parameters	8163/1/461	1365/0/78
Goodness-of-fit on F^2	0.802	1.060
Final R indexes [I>=2σ (I)]	R_1 = 0.0304, wR_2 = 0.0857	R_1 = 0.0549, wR_2 = 0.1716
Final R indexes [all data]	R_1 = 0.0309, wR_2 = 0.0866	R_1 = 0.0599, wR_2 = 0.1857
Largest diff. peak/hole / e Å^{-3}	0.32/-0.23	0.97/-0.50
Flack parameter	0.0075(17)	$C_{30}H_{24}F_{12}N_6NiP_2$

Table S2. Phase determination of $[M(bpy)_3](PF_6)_2$ crystals using single crystal X-ray diffraction.

M	Crystallization method	*a*	*c*	phase
Fe	MeCN evaporation	10.29(16)	16.0(2)	β
Fe	Acetone evaporation	10.83(4)	16.87(6)	β
Ni	Acetone evaporation	10.79(4)	16.58(6)	β
Ni	CH_2Cl_2 evaporation	10.76(2)	16.57(3)	β
Ni	CH_2Cl_2 evaporation	10.85(3)	16.69(4)	β
Ni	MeCN evaporation	10.74(8)	16.45(11)	β
Mn	CH_2Cl_2 evaporation	10.53(4)	26.53(11)	γ
Mn	Acetone evaporation	10.61(4)	26.79(11)	γ
Co	CH_2Cl_2 evaporation	10.63(13)	25.3(3)	γ
Co	MeCN evaporation	10.35(4)	26.21(11)	γ
Cu	MeCN evaporation	10.43(3)	26.30(6)	γ
Cu	Acetone evaporation	10.46(3)	26.38(7)	γ
Cu	CH_2Cl_2 evaporation	10.54(6)	26.53(15)	γ
Zn	Acetone evaporation	10.65(9)	26.9(2)	γ
Zn	MeCN evaporation	10.58(2)	26.62(6)	γ

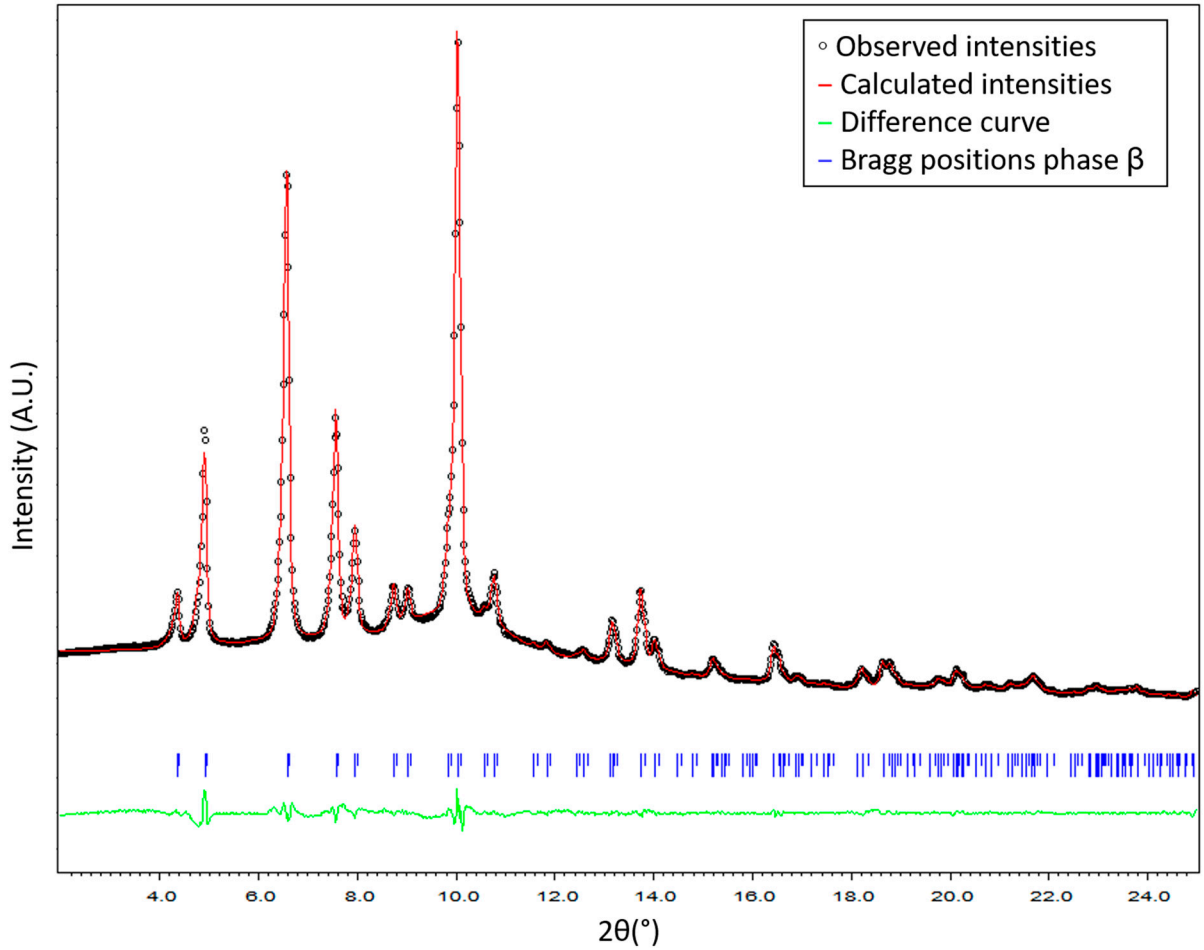

Figure S1. Profile matching refinement (Le Bail method) for ground single crystals of $[Ni(bpy)_3](PF_6)_2$ showing an unique β phase. Lattice parameters: a=b= 10.747(1) Å , c= 16.541(2) Å, α=β=90°, γ=120°. cwRp = 0.073; Goof = 2.53 (where cwRp is the background corrected wRp factor, MoKα_{12} radiation).

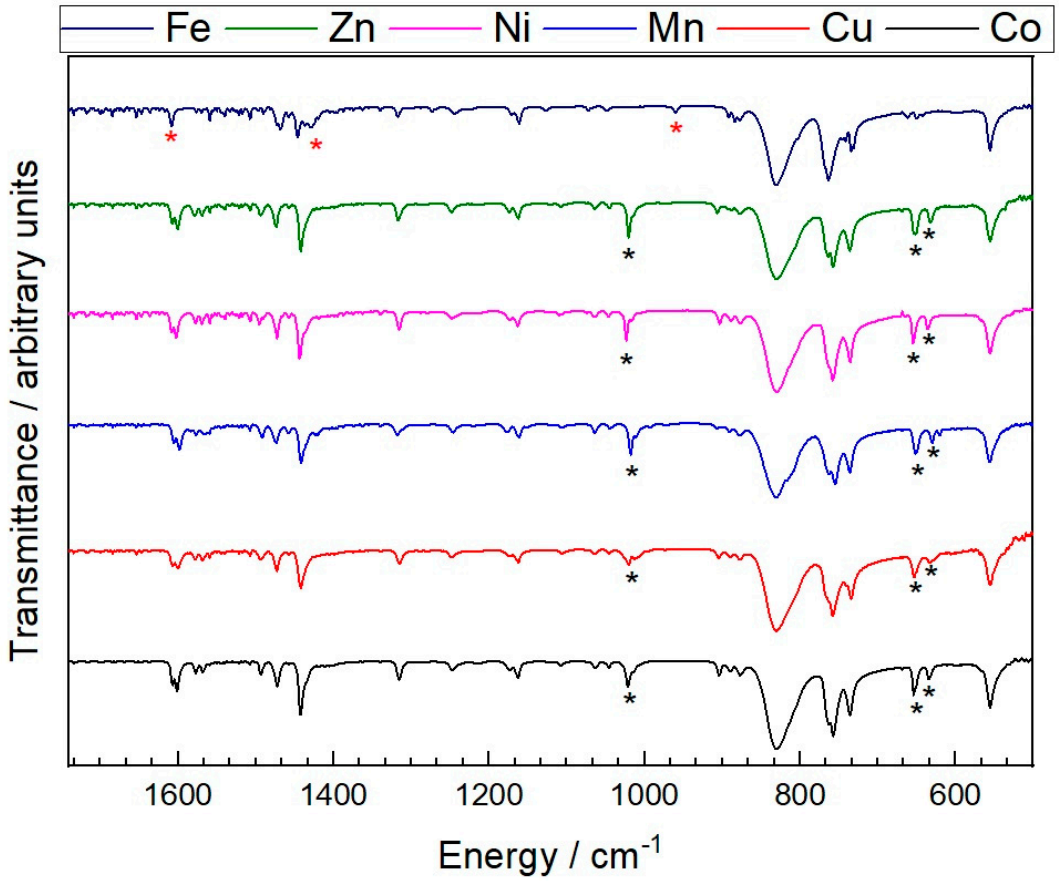

Figure S2. Infrared spectra of the precipitated powders. Peaks appearing only in the racemic phase denoted by red asterisk; peaks appearing only in the conglomerate phase denoted by black asterisks.

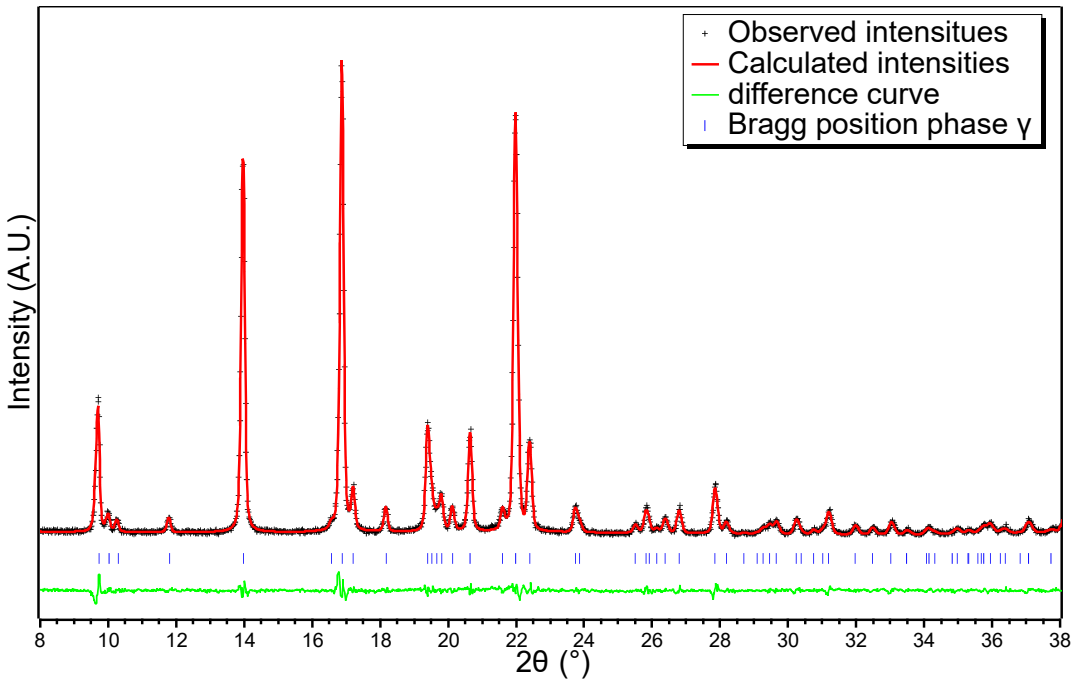

Figure S3. Profile matching refinement (Le Bail method) on the X-ray diffractogram for a co-precipitation of $[Ni(bpy)_3](PF_6)_2$ with $[Zn(bpy)_3](PF_6)_2$, showing an unique γ phase of $[Ni_xZn_{(1-x)}(bpy)_3](PF_6)_2$ for x = 0.3. cwRp = 0.11 ; Goof = 1.34 (where cwRp is the background corrected wRp factor, $CuK\alpha_{12}$ radiation).

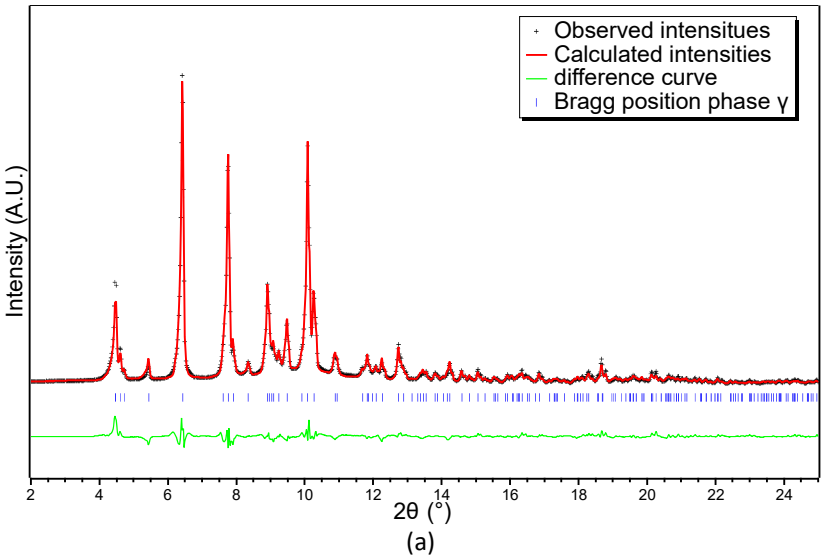

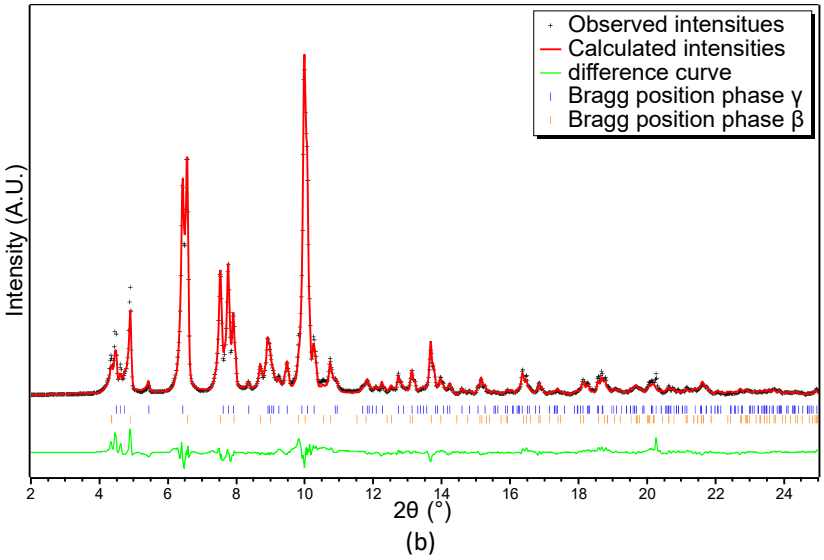

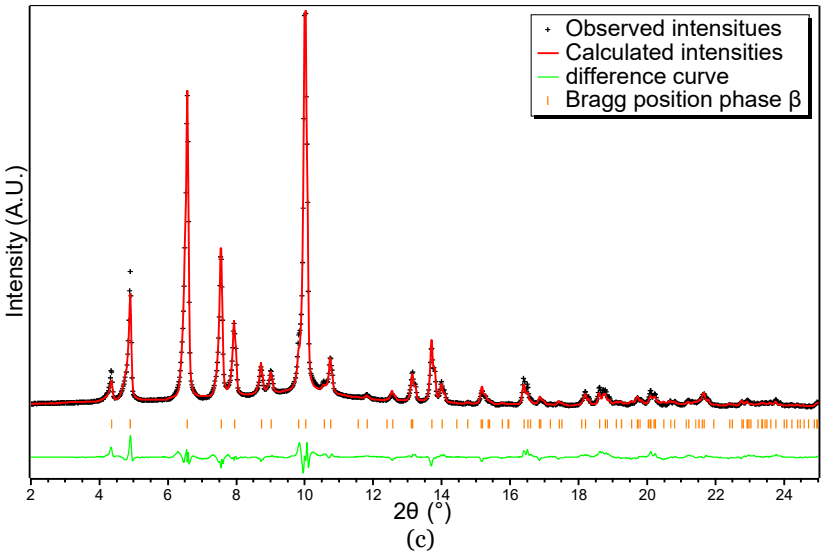

Figure S4. Rietveld refinement on X-ray diffractograms for ground single crystals of $[Ni_xZn_{1-x}(bpy)_3](PF_6)_2$ for **(a)** x = 0.1, showing an unique γ phase (cwRp = 0.12 ; wR2 = 0.09), **(b)** x = 0.4 showing a mixture of γ and β phases (cwRp = 0.13 ; wR2 = 0.10) and **(c)** for x = 0.9 showing an unique β phase (cwRp = 0.13 ; wR2 = 0.13) . cwRp is the background corrected profile reliability factor and wR2 the structural reliability factor.

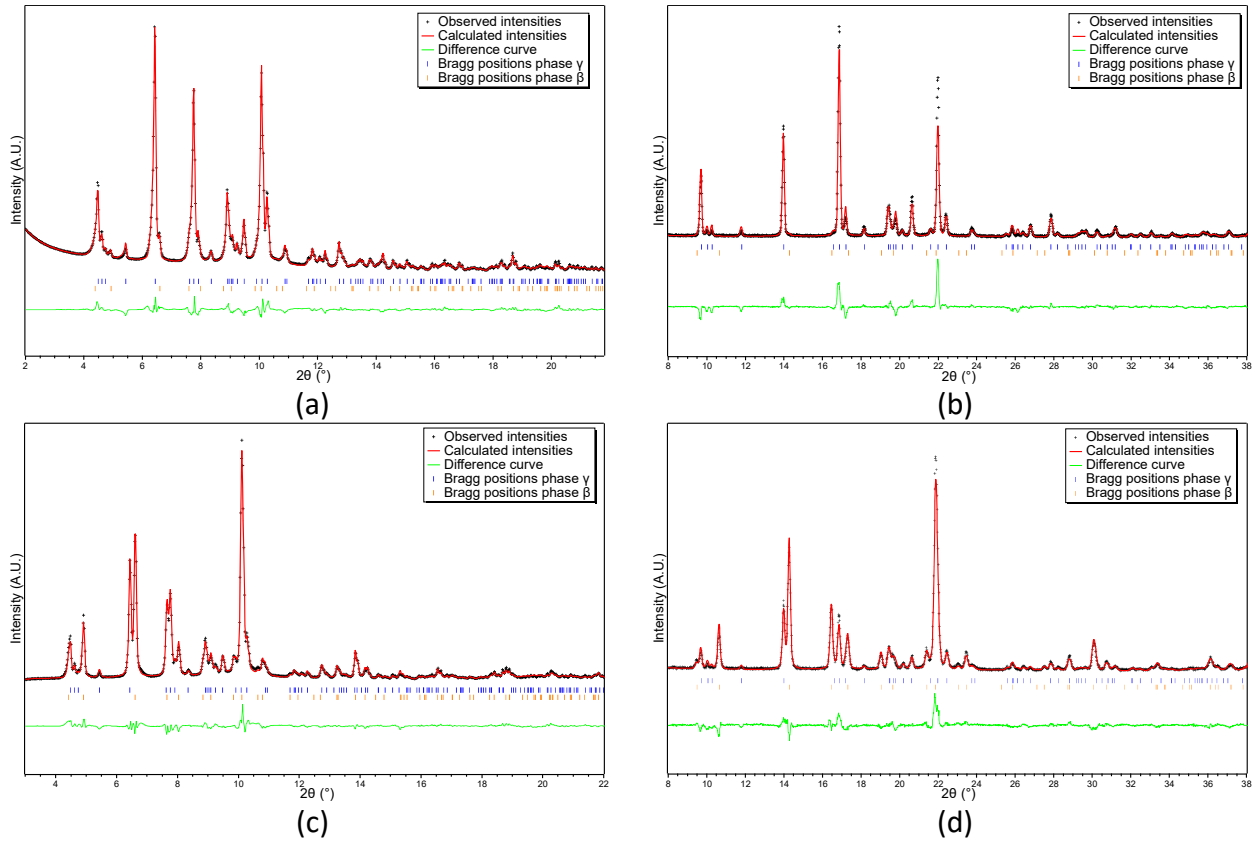

Figure S5. Rietveld refinement on X-ray diffractograms for ground single crystals **(a)** and **(c)** and powders **(b)** and **(d)** of $[Fe_xZn_{1-x}(bpy)_3](PF_6)_2$ showing a mixture of γ and β phases for (a) and (b) : x = 0.1 and % β = 7% and 1% respectively and (c) and (d) : x = 0.4 and % β = 54% and 65% respectively. (a) cwRp = 0.10 ; wR2 = 0.08 ; (b) cwRp = 0.27 ; wR2 = 0.16 ; (c) cwRp = 0.11 ; wR2 = 0.08 ; (d) cwRp = 0.20 ; wR2 = 0.09 (where cwRp is the background corrected profile reliability factor and wR2 the mean structural reliability factor, MoKα_{12} radiation for ground single crystals and CuKα_{12} radiation for powders).

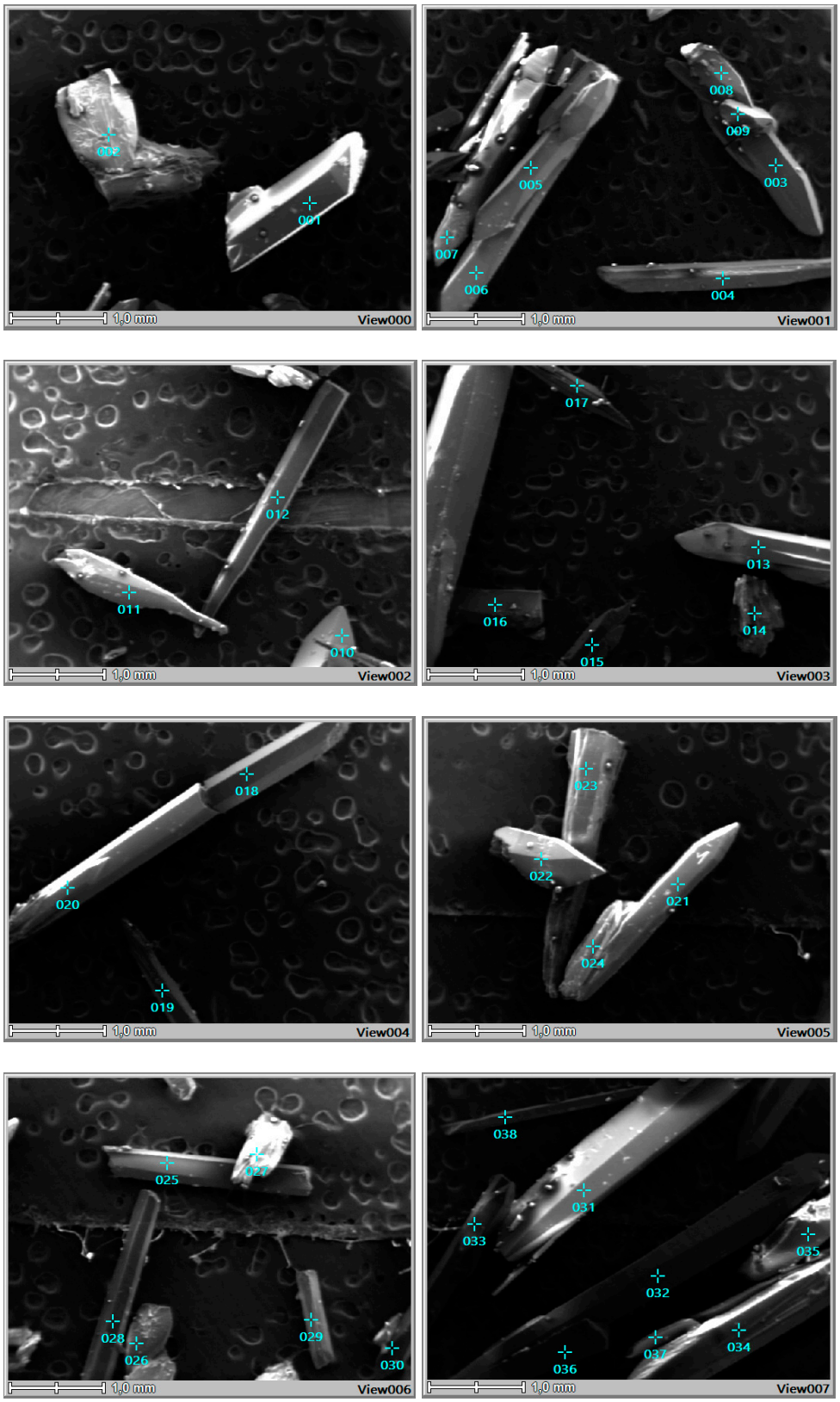

Figure S6a. SEM images of $[Ni_{0.4}Zn_{0.6}(bpy)_3](PF_6)_2$. Blue crosses show the point where metal content was assayed by EDX. See table S3 for metal assay at the labeled points.

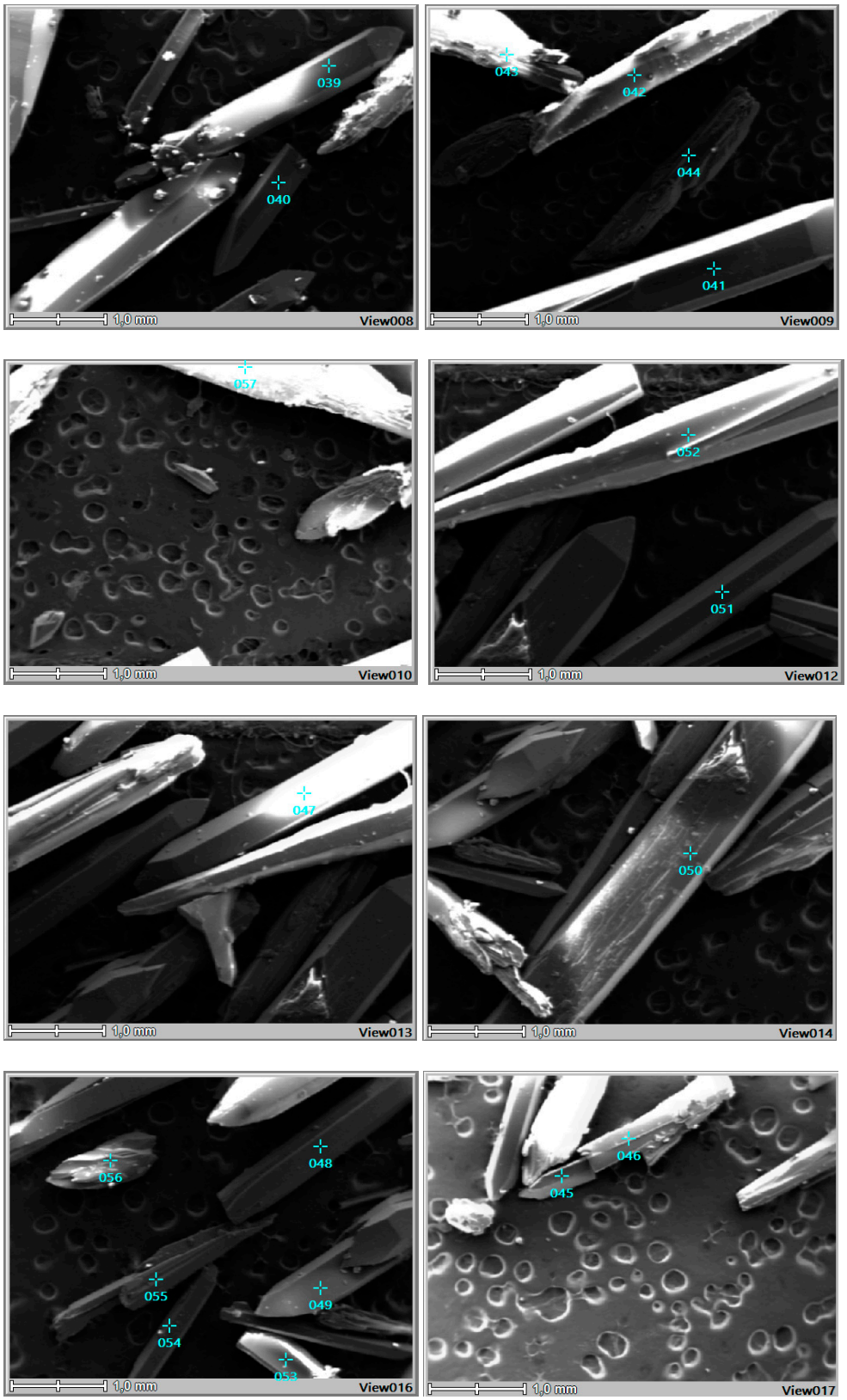

Figure S6b. SEM images of $[Ni_{0.4}Zn_{0.6}(bpy)_3](PF_6)_2$. Blue crosses show the point where metal content was assayed by EDX. See table S3 for metal assay at the labeled points.

Table S3. Nickel and zinc proportions measured by EDX at the points corresponding to the blue crosses in Figures S6a and S6b.

Marker	Ni At%	Zn At%	Marker	Ni At%	Zn At%
1	37.10	62.90	30	43.29	56.71
2	57.00	43.00	31	35.56	64.44
3	25.97	74.03	32	28.94	71.06
4	55.83	44.17	33	27.79	72.21
5	32.99	67.01	34	58.01	41.99
6	28.78	71.22	35	37.83	62.17
7	30.95	69.05	36	51.36	48.64
8	24.76	75.24	37	66.60	33.40
9	30.47	69.53	38	49.37	50.63
10	28.50	71.50	39	64.40	35.60
11	40.97	59.03	40	30.17	69.83
12	33.78	66.22	41	36.35	63.65
13	36.28	63.72	42	37.57	62.43
14	46.73	53.27	43	57.15	42.85
15	44.10	55.90	44	49.40	50.60
16	53.24	46.76	57	56.05	43.95
17	62.27	37.73	51	34.40	65.60
18	33.48	66.52	52	36.94	63.06
19	59.21	40.79	47	37.26	62.74
20	31.74	68.26	50	53.36	46.64
21	38.07	61.93	48	57.58	42.42
22	28.00	72.00	49	30.84	69.16
23	52.37	47.63	53	61.23	38.77
24	56.64	43.36	54	66.55	33.45
25	29.14	70.86	55	41.82	58.18
26	36.54	63.46	56	36.70	63.30
27	35.77	64.23	45	58.54	41.46
28	45.76	54.24	46	48.58	51.42
29	61.24	38.76			

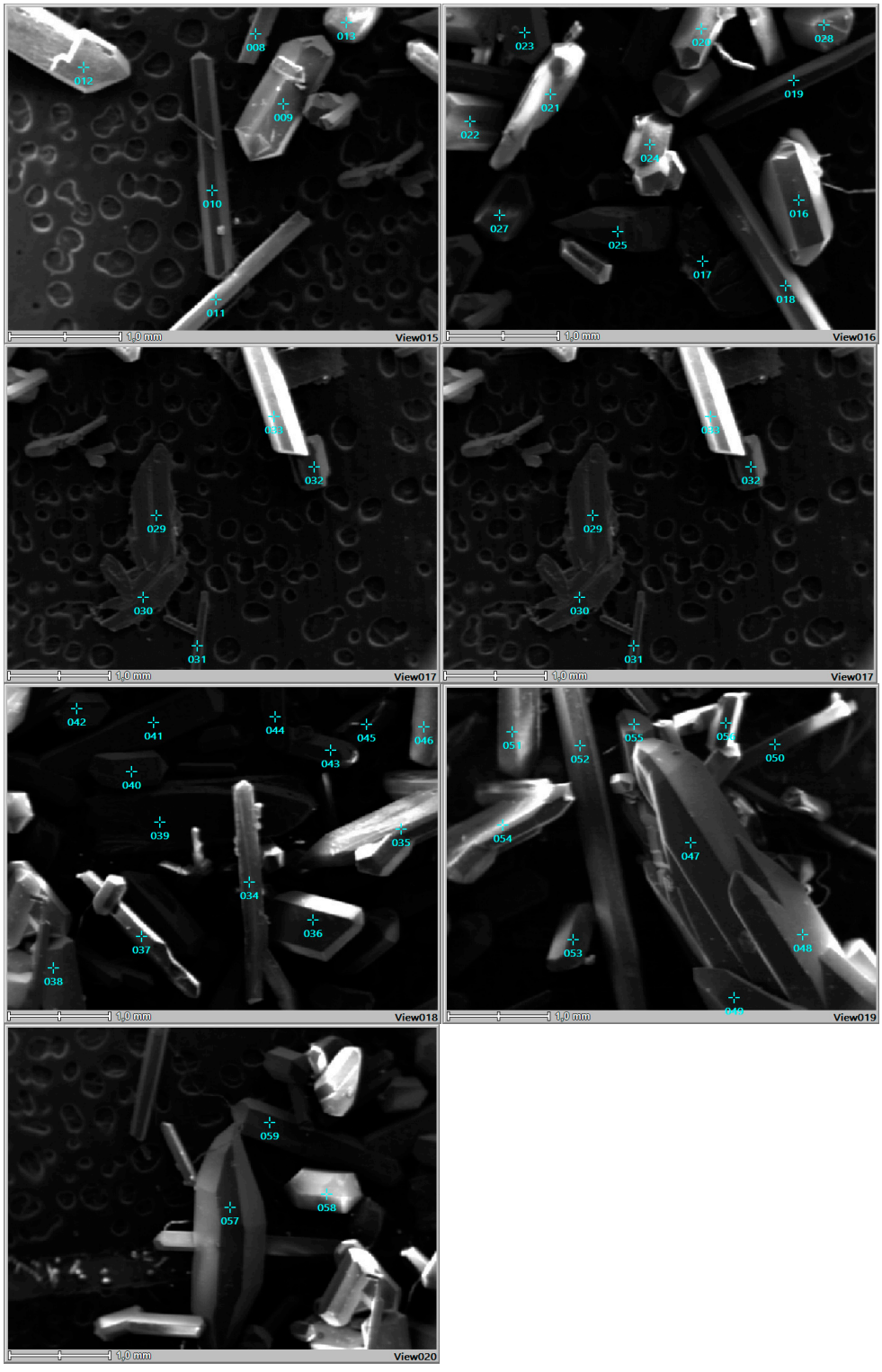

Figure S7. SEM images of $[Fe_{0.5}Zn_{0.5}(bpy)_3](PF_6)_2$. Blue crosses show the point where metal content was assayed by EDX. See table S4 for metal assay at the labeled points.

Table S4. Nickel and zinc proportions measured by EDX at the points corresponding to the blue crosses in Figure S7.

Marker	Fe At%	Zn At%	Marker2	Fe At%3	Zn At%
7	58.07	41.93	36	71.56	28.44
8	70.65	29.35	37	69.58	30.42
9	88.89	11.11	38	70.87	29.13
10	62.11	37.89	39	2.52	97.48
11	62.92	37.08	40	72.24	27.76
12	77.07	22.93	41	58.53	41.47
13	85.24	14.76	42	63.87	36.13
16	64.47	35.53	43	69.44	30.56
17	5.30	94.70	44	74.75	25.25
18	2.94	97.06	45	64.81	35.19
19	81.46	18.54	46	54.49	45.51
20	65.01	34.99	47	2.42	97.58
21	4.96	95.04	48	2.45	97.55
22	89.09	10.91	49	1.83	98.17
23	73.73	26.27	50	55.46	44.54
24	67.66	32.34	51	71.13	28.87
25	3.42	96.58	52	57.04	42.96
27	63.9	36.10	53	65.81	34.19
28	66.39	33.61	54	6.13	93.87
29	1.37	98.63	55	59.29	40.71
30	0.91	99.09	56	60.52	39.48
31	81.27	18.73	57	2.74	97.26
32	72.23	27.77	58	74.75	25.25
33	59.62	40.38	59	58.63	41.37
34	61.32	38.68			

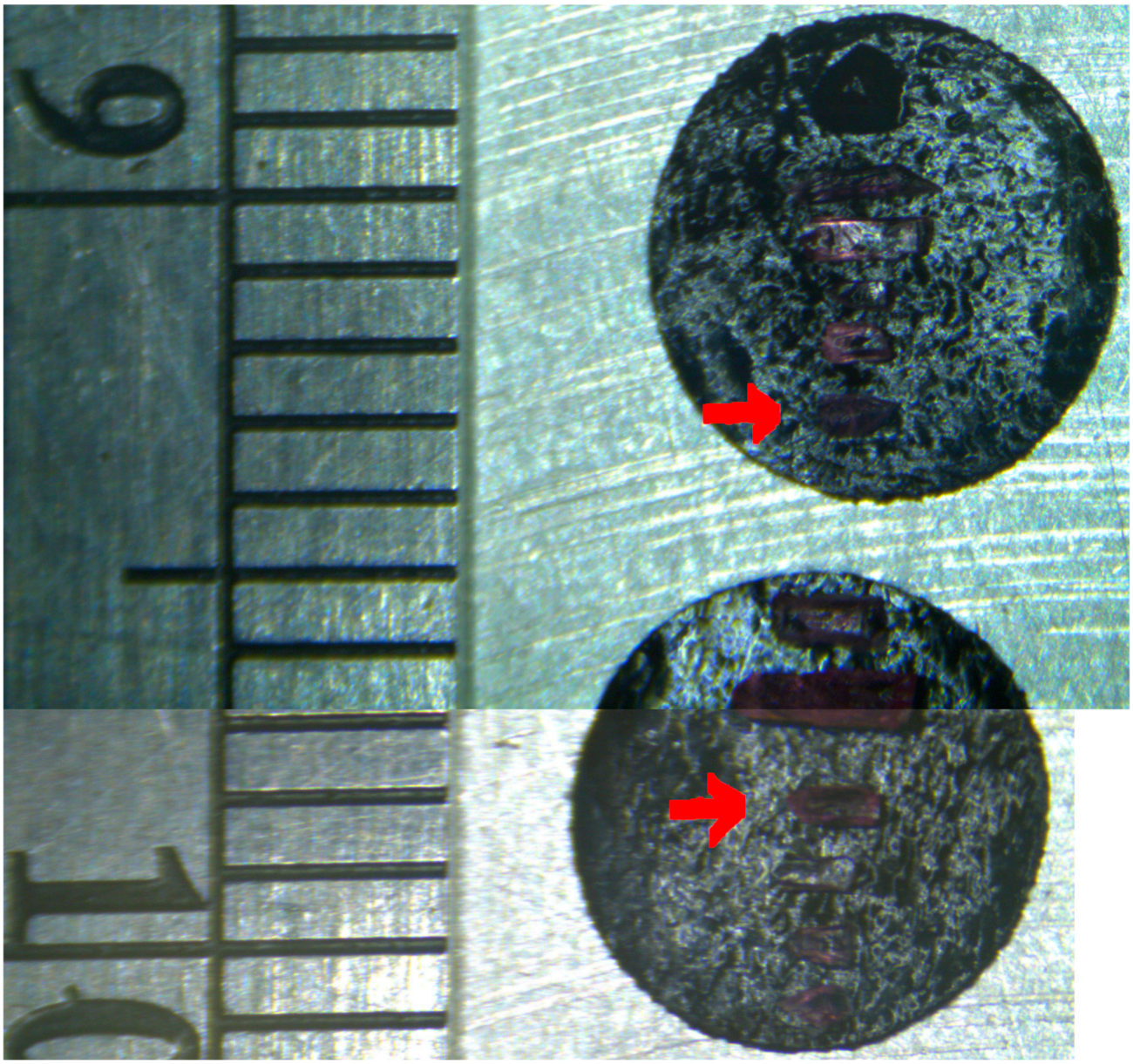

Figure S8. Sample mounting for X-ray Natural Circular Dichroism, crystals were glued to carbon tape pads with the *c* axis lying horizontal. The sample holder can be rotated along the vertical of the representation, with the X-ray beam normal to the picture. Measurements reported herein were performed on the crystals indicated by the red arrows.

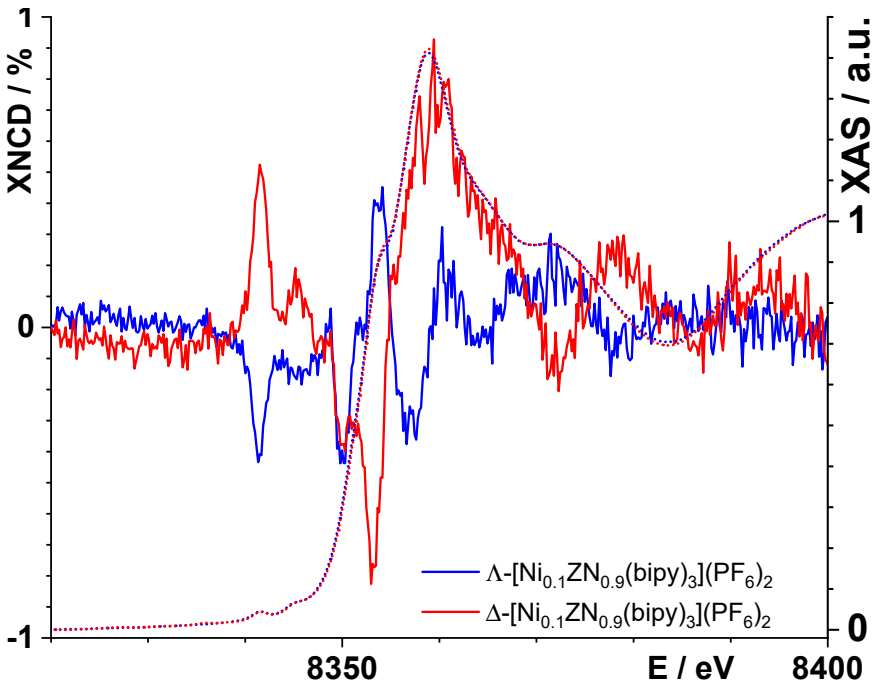

Figure S9. Absorption (dotted lines) and XNCD (full lines) spectra for single crystals, in orthoaxial configuration respective to the beam, for the Δ (in red) and Λ (in blue) enantiomers of $Ni_{0.1}Zn_{0.9}(bpy)_3(PF_6)_2$. EDX measurements on both enantiomers gave proportions of $Ni_{0.106}Zn_{0.894}$ for Δ and $Ni_{0.12}Zn_{0.88}$ for Λ.

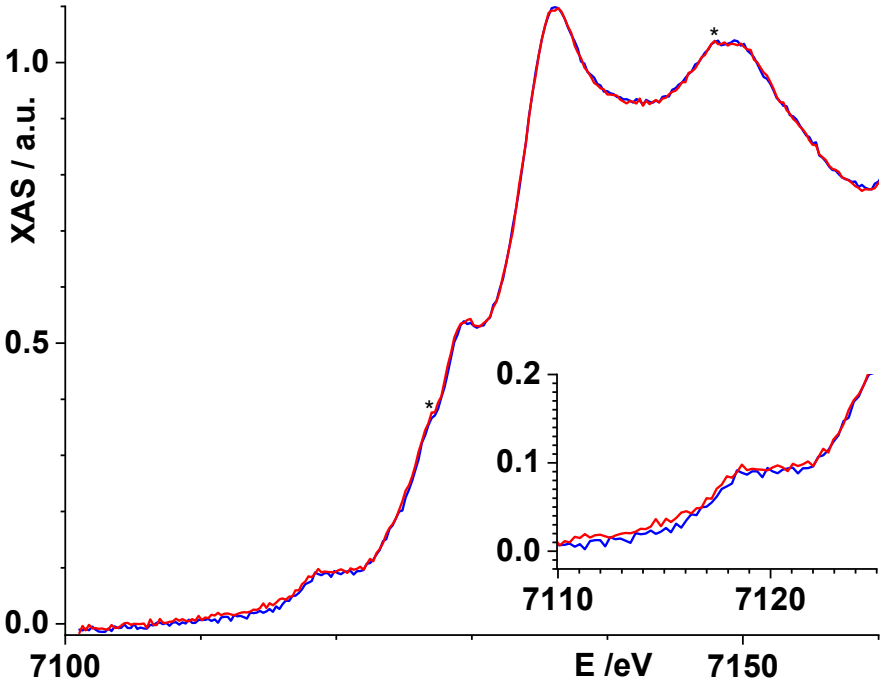

Figure S10. X-ray absorption spectra for both circular polarizations of the beam (red and blue lines) on a single crystal of the Δ enantiomer of $Fe_{0.1}Zn_{0.9}(bpy)_3(PF_6)_2$, in orthoaxial configuration respective to the beam. Diffraction peaks present in this pair of spectra are signaled with a *. (inset) zoom on the pre-edge region.